

# EXTENSIVE METRIC PERFORMANCE EVALUATION OF A 3D RANGE CAMERA

Christoph A. Weyer<sup>3</sup>, Kwang-Ho Bae<sup>1,2,\*</sup>, Kwanthar Lim<sup>1</sup> and Derek D. Lichti<sup>4</sup>

<sup>1</sup>Western Australian Centre for Geodesy & The Institute for Geoscience Research, Department of Spatial Sciences, Curtin University of Technology, GPO Box U1987, Perth, WA 6845, Australia

<sup>2</sup>Cooperative Research Centre for Spatial Information (CRC-SI), Australia

<sup>3</sup>Institut für Photogrammetrie und Fernerkundung, Universität Karlsruhe (TH), Karlsruhe, Germany

<sup>4</sup>Department of Geomatics Engineering and Centre for Bioengineering Research and Education, University of Calgary, Calgary, Canada

- k.h.bae@curtin.edu.au, - weychr@gik.uni-karlsruhe.de, - kwanthar.lim@student.curtin.edu.au, - ddlichti@ucalgary.ca

## Commission V, WG 3

**KEY WORDS:** Range camera, Calibration, Measurement error, Performance analysis

## ABSTRACT:

Three dimensional (3D) range cameras measure 3D point clouds and intensity information of objects using time-of-flight methods with a CMOS/CCD array. Their emerging applications are security, surveillance, bio-mechanics and so on. Since they comprise a CMOS/CCD array, a nearest-neighbor search for individual points is not necessary, which can increase the efficiency in estimating the geometric properties of objects. This fact leads us to broaden the application areas of 3D range cameras to real-time and dynamic applications such as mobile mapping and vehicle navigation. This paper presents extensive metric performance tests of a 3D range camera (SwissRanger SR-3000). It is composed of a 176x144 pixel CMOS array for which the pixel size and spacing are both 40µm. The nominal principal distance of the lens is 8mm. Several rangefinder system parameters such as the integration time and the modulation frequency can be set by the user. For example, the shorter integration time is maximising the signal-to-noise ratio. In addition, the maximum unambiguous range is 7.5m with the modulation frequency of 20MHz.

## INTRODUCTION

Three dimensional (3D) range cameras measure 3D point clouds and intensity information of objects using time-of-flight methods with a CMOS/CCD array. Their emerging applications are security, surveillance, bio-mechanics and so on. Since they comprise an array of small detectors, a nearest-neighbor search for individual points is not necessary for the case of single instrument, which can increase the efficiency in estimating the geometric properties of objects. This fact leads us to broaden the application areas of 3D range cameras to real-time and dynamic applications such as mobile mapping and vehicle navigation.

It is a new and largely untested technology showing potential in industrial applications. In general, a laser scanner would be used to obtain 3D coordinates of an object, which may be unsuitable in conditions having spatial and temporal limitations and financial constraints. Therefore, a range camera may provide a more suitable alternative, taking for example the automotive industry where 3D range cameras' size allows it to be mounted in the interior of the car to observe passenger position as part of the airbag sensing systems (Oggier et al., 2005). In order to ensure a good metric performance in these applications, it is necessary to evaluate the camera to highlight the areas of promise and areas that need further development, such as calibration and error modelling. Errors need to be identified by first conducting experiments to analyse basic elements of the camera used in those industries, beginning here with its accuracy and precision.

This paper provides a general overview of this new instrument and extensive metric performance tests of a 3D range camera, SwissRanger SR-3000 (Mesa Imaging, 2008).

## BACKGROUND

Images from current cameras display only two dimensions (2D), lying in the x and y coordinate space. In order to obtain three-dimensional (3D) information, photogrammetry techniques using two images of the same place from differing perspectives will allow 3D coordinates to be computed.

There are three types of non-contact distance measurement methods such as triangulation, interferometry and time-of-flight (Buttgen et al., 2005; Gordon, 2005). A 3D range camera used in this study, SwissRanger SR-3000 (Mesa Imaging, 2008), is based on the time-of-flight principle using a continuous wave modulation (Buttgen et al., 2005; Kahlmann et al., 2006; Karel et al., 2007). The continuous wave modulation system is frequently used on 3D range cameras. As shown in Figure 1, a sinusoidal signal is transmitted toward the scenery or an object, which is reflected and received by a sensor, such as a charge-coupled device (CCD) array. The range is then estimated using the phase differences between the emitted and received sinusoidal signals. The phase shift,  $\varphi$ , between the transmitting and returning signal is given as

$$\varphi = \tan^{-1} \left( \frac{c(\tau_3) - c(\tau_1)}{c(\tau_0) - c(\tau_2)} \right) \quad (1)$$

\* Corresponding author

and the distance between the range camera and an object,  $d$ , is estimated as

$$d = \frac{\lambda_{\text{mod}}}{2} \frac{\varphi}{2\pi} \quad (2)$$

where  $\lambda_{\text{mod}}$  is the modulation wavelength. This technology allows 3D data to be captured simultaneously, as well as removing the requirement to capture two images for processing. Therefore, it reduces the necessity to have multiple setups and perhaps increases the efficiency for post processing of the images.

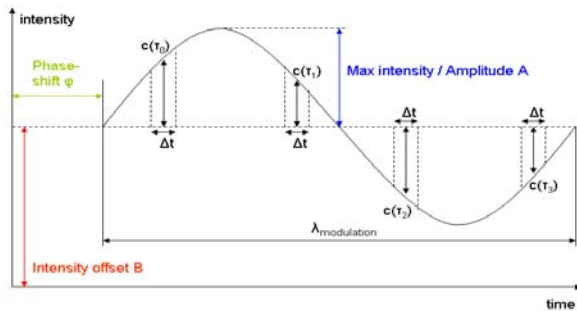


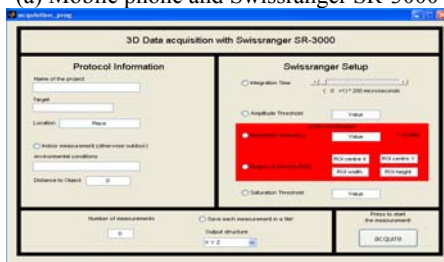
Figure 1. Phase shift distance measurement principle for 3D range cameras where  $c(\tau_i)$  is the detected intensity of the returned signal at time  $\tau_i$  and  $\Delta\tau$  is the temporal sampling interval of a 3D range camera.

### 2.1 Swissranger SR-3000 Camera

The Swissranger SR-3000 camera is composed of a 176x144 pixel CMOS array for which the pixel size and spacing are both 40µm. The nominal principal distance of the lens is 8mm. Several rangefinder system parameters such as the integration time (max. 51.2ms) and the modulation frequency can be set by the user. For example, the shorter integration time is maximising the signal-to-noise ratio. In addition, the maximum unambiguous range is 7.5m with the modulation frequency of 20MHz (Mesa Imaging, 2008).



(a) Mobile phone and Swissranger SR-3000



(b) Matlab-based interface

Figure 2. SwissRanger SR-3000 camera. A simple Matlab-interface for a SwissRanger SR-3000 was written by Christoph Weyer and Kwanthar Lim.

LEDs (Light Emitting Diode) are favoured over conventional lasers since they can produce a continuous wave with a high modulation frequency and a low price. SwissRanger SR-3000 has 55 LEDs with a modulation frequency of 20MHz and a wavelength of 870nm. The field of view is round about 47.5°x 39.6° and the special resolution about 1cm in a distance of 1m. In front of the sensor, an optical band-pass filter is placed in order to reduce the impact of background illumination (Oggier et al., 2003). More details on the hardware aspects of SwissRanger SR-3000 can be found in Lange et al (2000) and Oggier et al. (2003).

### 2.2 Potential applications

The use of 3D image capture technology has already been implemented in the area of robotics. As shown in Weingarten et al. (2004), the preceding model of the SRC is mounted on the robot for path planning and objects recognition. Weingarten et al. (2004) also demonstrates a 3D camera's advantage over the use of laser scanning when it comes to object recognition and stopping distance.

The automotive industry can use it for determining airbag initialisation times and other safety features (Oggier et al. 2005). The compact size and low power requirements (Mesa Imaging 2008) allow the 3D camera to be placed in almost any location, as seen in Figure 5 it is mounted near the rear view mirror. This 3D capture technology would be used to take a snapshot of body features for biometrical applications. Laser scanners are generally set up for the mapping of body features, but the 3D camera provides both 2D and 3D data all within the single device at a comparatively cheaper cost and using a much smaller device (Oggier et al. 2005). An interactive screen for gaming and presentations may be the future technological enhancements to replace the use of keyboard and mouse setups to favour the implementation of a 3D camera, providing the camera becomes available at the consumer level. Development of this virtual interaction has started which can be seen in the paper by Oggier et al. (2005) where a game of snake being played.

Some applications that may allow the use of such a device in this industry include interior building surveys to determine the inner dimensions of the room, with a benefit of locating all necessary objects with one camera setup instead of using many tape measurements. There is a possibility for use in underground mining, building on the idea of robotic applications to create a remote controlled robot to take images of stopes, mineshafts and other hazardous locations, not only providing images of the areas, but also allowing 3D models to be constructed with the data.

## EXPERIMENT I

### 3.1 Experimental setup

First we conducted a simple experiment for the residual analysis of the first order plane fitting with two targets with different colours and the size of 50cm by 50cm. The SwissRanger SR3000 was mounted on a tripod and the target was mounted on a stable heavy weighted stand as shown in Figure 3a. A matte white target is shown in Figure 3b. Note that the z-axis of the range camera is defined as the direction from the camera to the target and so the x- and y- axes of the measured coordinates are parallel to the tangential surface of the target accordingly.

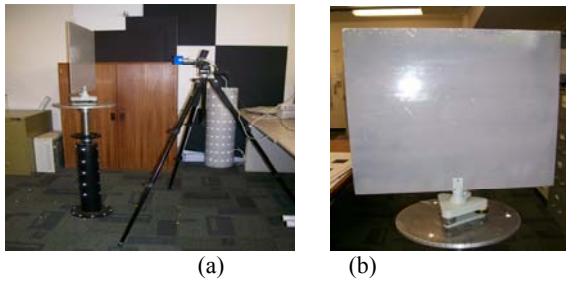


Figure 3. Simple experimental setup for the residual analysis of a flat target with two different colours.

### 3.2 Precision assessment

The residual plots of two targets, matte black and white targets, are shown in Figure 4 with respect to the range from the centre, which is defined as the distance of a point from the centre of a test flat target. The nominal distance between the range camera and the targets is 50cm. These figures show that the precision of the measure points are decreased as the range from the centre increases. In addition, the rate of the decrement for the matte black target is larger than that of the matte white target. The maximum residuals of the first order least-squares fitting are 8cm and 4cm for the matte black and whites targets, respectively. In addition, a larger number of gross outliers are observed in the boundaries of both targets. This demonstrates that the precision performance of this range camera is largely dependent on the radiometric characteristics of an object, i.e. the strength of the returned intensity by the object.

The residuals of the first order plane fitting are also presented in Figure 5 with respect to the x-axis of the measurement, which is parallel to the surface of the flat test targets. These patterns again show the same result as Figure 4. In particular, a large amount of gross outliers were observed from the residual pattern at the centre of the matte white target, i.e. Figure 5b. This is resulted from a strong intensity return from the centre of the target because of the nominal incidence angle at this part of 90° and its colour, i.e. white.

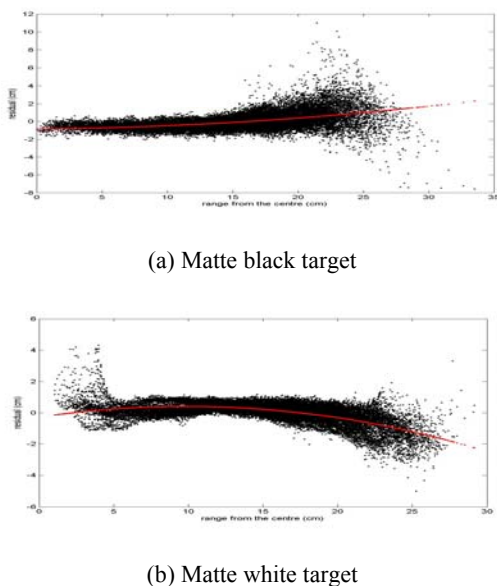
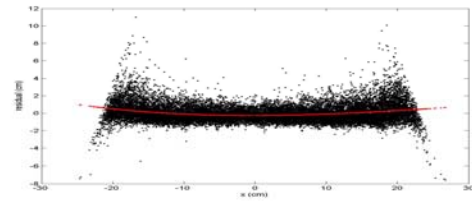
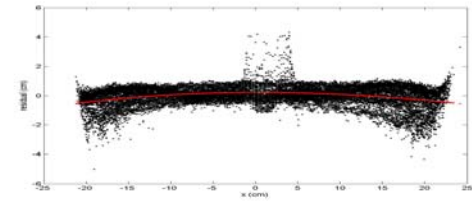


Figure 4. Residual vs. the range from the centre which is defined as the distance of a point from the centre of the target.



(a) Matte black target

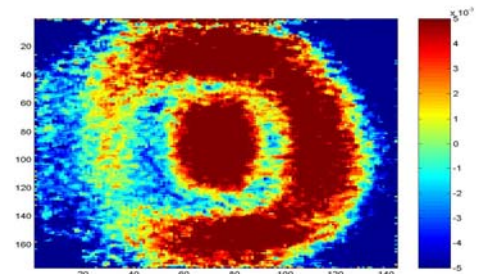


(b) Matte white target

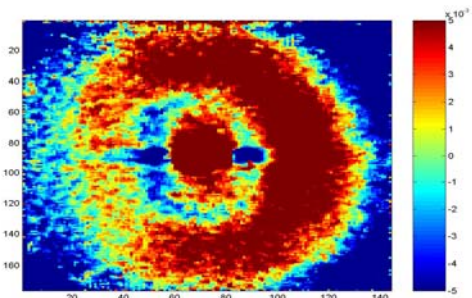
Figure 5. Residual vs. the x-axis that is parallel to the tangential surface of the test target.

### 3.3 Residual pattern analysis

In this section, as another tool for the precision assessment, two-dimensional (2D) colour plots of the residual patterns are presented in Figure 6. In other words, the residual of the first order plane fitting were transformed to the 2D image space of the range camera, i.e. 176x144.



(a) Matte black target



(b) Matte white target

Figure 6. Residual pattern plots (matte white). (a) The nominal distance between the range camera and the matte black target is 25cm. (b) The distance of the matte white target from the camera is approximately 50cm. The unit of colour bar is metres.

The 2D residual patterns of the matte black target are presented in Figure 6. The distances between the targets and the range camera for Figures 6a and 6b are approximately 25cm. In Figure 6a, two abnormal residual patterns are observed. First, a high residual is shown in the boundary of the target, which was observed in Figures 4 and 5 in the previous section. Second, in the centre of the matte black target, the same amount of the residual as the target's boundary is observed and it is caused by the higher returned intensity than the case of the Figures 4 and 5 since the distance of the camera and the target is shorter. In Figure 6b, the residual pattern of the matte white target at the distance of 50cm presents the same pattern as the matte black target in Figure 6.

## EXPERIMENT II

As the second part of the experiments for this paper, we conducted several precision tests with various hardware setup such as warm-up time, integration time and amplitude threshold. As an example, the intensity and range images from SwissRanger SR-3000 are presented in Figure 7 with the distance threshold (minimum distance = 1.80m and maximum distance = 2.20m).

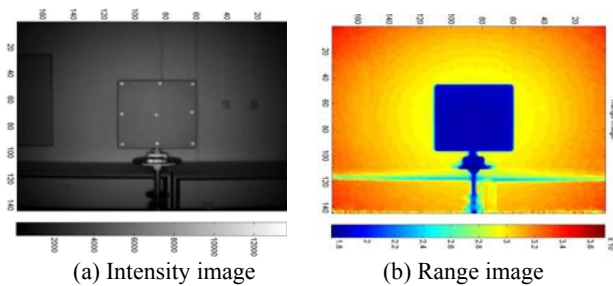


Figure 7. Intensity and range data from SwissRanger SR-3000.

### 1.1 Warm-up time

For the test on the warm-up time, the distance of the target from the camera was approximately 1m and the same setup as Figure 3a with a flat target with grey colour was utilized. A continuous measurement was conducted for 8 minutes. The interval between each measurement was 1.5 seconds and 20 seconds pause after every minute. The estimated distance by the first order plane fitting and the mean intensity of the target are presented in Figure 8 with respect to the measurement time.

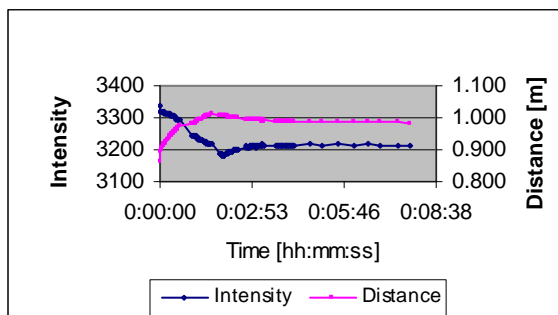


Figure 8. Warm-up time vs. Mean intensity and the estimated distance of a flat target from the range camera.

After turning on the range camera, the estimated distance increases within the time window of about 2 minutes as shown in Figure 8. The approximate accuracy error is about 10cm within 2 minutes after the starting of the measurement. Further more, a relationship between the measured intensity and the accuracy of the range camera as shown in Figure 8. In other words, its bias in the distance measurement is directly related to the warming up of the camera. From our experiment, the minimum warming-up time of 6 minutes is recommended.

### 1.2 Repeatability

Before the metric performance tests with both integration time and amplitude threshold of SwissRanger SR-3000, we conducted a test on the repeatability or reliability test of the range camera. To do this, we conducted a successive 30 measurements in the different distances of the target, from 1m to 4m, with interval of 1m. The mean estimated distance of the 30 measurements was utilised to calculate a reference distance, named  $D_{mean}$ . In Figure 9, the difference between the distance of the estimated distance of each measurement and  $D_{mean}$  is presented. For the cases of the distances of the target from the range camera (100cm, 200cm and 300cm), the standard deviation of the difference from  $D_{mean}$  is within 2mm. In the case of 400cm, the standard deviation of the difference from  $D_{mean}$  is about 1cm.

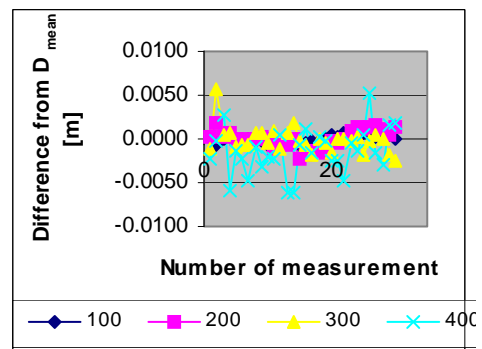


Figure 9. Difference from the mean distance ( $D_{mean}$ ) with various target-camera distances from 100cm to 400cm.

### 4.3 Integration time

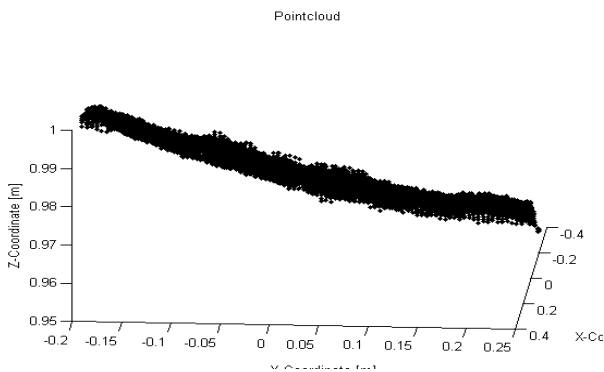
In this section, some test results on the integration time will be presented, which is one of the most important parameters of a range camera such as SwissRanger SR3000. In order to obtain knowledge about setting the right or optimal integration time, a grey metal target were used. In addition, in order to a reliable measurement, a total amount of 30 measurements were recorded for every setting and were averaged for the least squares adjustment.

Two plots of 3D point clouds from the grey flat target with two different integration times, 20ms and 51ms are presented in Figure 10, as an example of the important of the integration time for a range camera. Around the centre of the target, we can observe some erroneous measurement by the range camera.

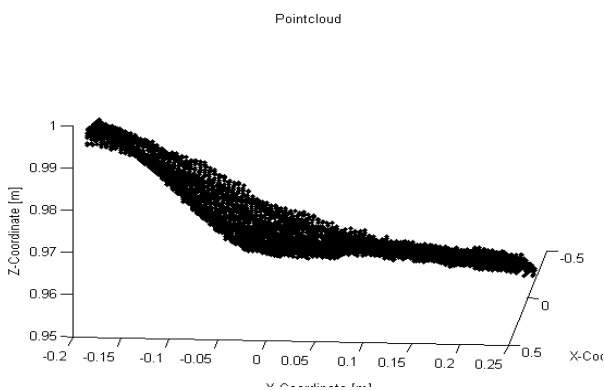
Markers were placed on the ground in a distance of 0.10, 0.25, 0.50, 0.70, 1.00, 1.25, 1.50, 3.00, 3.50, 4.00, 5.00m measured from the back side of SwissRanger SR3000. The target moved from one marker to another after every measurement. Note that

the numbers of the image pixels belongs to the targets decrease as the distance of the target increases. On every position the integration time was set up from 200 $\mu$ s to 51.2ms in 2000 $\mu$ s intervals, except of the distances 0.10m, 0.25m, 0.50m and 0.70m. Furthermore, air temperature was controlled with an air conditioning system in the laboratory in order to assure almost the same air temperature conditioning for each measurement as much as we could.

Figure 11 presents the standard deviation of the first order plane fitting with various distances of the target from the range camera with respect to different integration time. First, a greater dependency of the measurement precision is observed on the integration time in the shorter distance, 25cm to 70cm, as shown in Figure 11a. In this range of the distance, i.e. smaller than 70cm, the maximum difference in the measurement precision is about 600%. In addition, in the medium range of the distance, 1m to 1.5m, this effect is much smaller but the maximum difference in the measurement precision is still as large as 150% as shown in Figure 10b. Third, as we can observed in Figure 11c, the importance of an optimal integration time is much less important in a long distance of the target from the range camera. In other words, there is a large size of basin in the integration time, about 30ms, where any integration time provides as large as the standard deviation of the residual, 1cm.

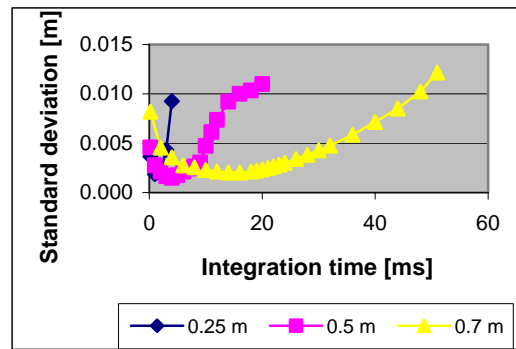


(a)  $T_{\text{Integration}} = 20\text{ms}$

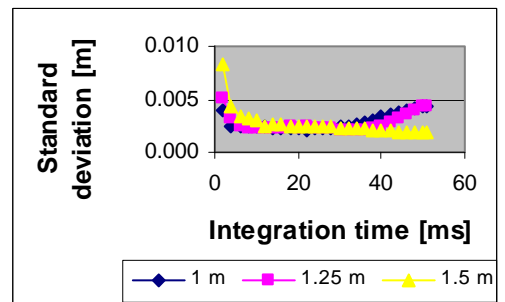


(b)  $T_{\text{Integration}} = 51.2\text{ms}$

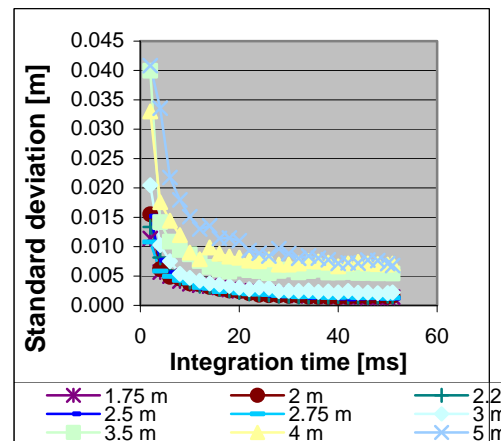
Figure 10. Measured 3D point clouds with different integration time ( $T_{\text{Integration}}$ )



(a) Short distances



(b) Medium distances



(b) Distances between 1.75m and 3m

Figure 11. Standard deviation of the residuals vs. the integration time with various distances of the target.

### 1.3 Amplitude threshold

The last parameter to be tested is the amplitude threshold. The amplitude of a range camera is measured from the amount of emitted light that is reflected back on the pixel of the camera, which means it can qualify the measurement for each pixel. A pixel of the camera's detector with a lower amplitude value than the threshold can be filtered out by a threshold value. There is a lot of background illumination, which could influence the distance measurement of the target, especially at the corners of an object. As an example, in Figure 12b, whole background was eliminated (blue colour in Figure 12a) and only the target with its tripod remained.

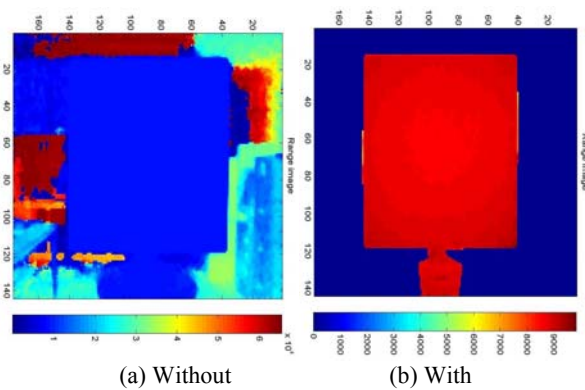


Figure 12. Range image without and with amplitude threshold

A test on amplitude threshold was conducted with various integration times using the grey flat target and the estimated distance with the nominal distance of the target to the range camera of 1m. We observed a little effect on the measurement precision, i.e. the standard deviation of the residual, by amplitude threshold. However, in terms of its accuracy, amplitude threshold provided a better measurement accuracy as shown in Figure 13.

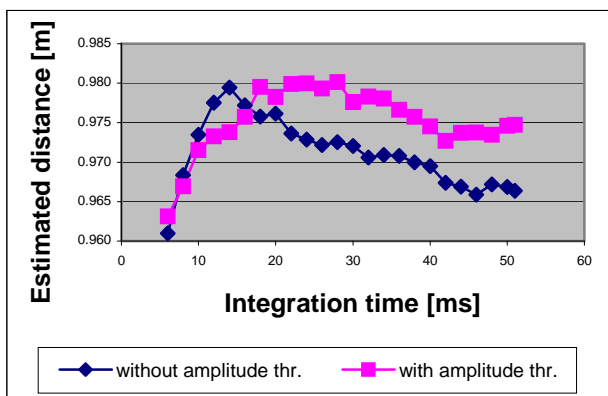


Figure 13. Estimated distance with and without amplitude threshold vs. Integration time

### CONCLUDING REMARKS

Metric performance of a 3D range camera, SwissRanger SR-3000, was extensively evaluated in terms of its precision and its hardware setting values such as warming-up time, integration time and amplitude threshold.

We reported that a large variation in the measurement precision within the distance of an object to the camera smaller than 70cm. In addition, in the case of a distance greater than 1.75m, the integration time of 30ms provides a maximum of 1cm precision. However, note that all the experiments in this paper were conducted with a flat target, not with general objects. In addition, we recommend users to use a photogrammetric calibration method to remove a lens distortion effect as shown in Figure 6, which will be our future works on this new photogrammetry tool.

A simple Matlab-GUI SwissRanger Interface program used in this paper is freely available for research-related works. If any

one is interested, please contact either Kwang-Ho Bae or Christoph Weyer.

### ACKNOWLEDGEMENTS

This work has been in part supported by the Cooperative Research Centre for Spatial Information, whose activities are funded by the Australian Commonwealth's Cooperative Research Centres Programme. The first author thanks to The Institute for Geoscience Research (TIGeR) at Curtin University of Technology for a travel grant.

We thanks to Mr David Belton for his assistance on a diploma project by C. Weyer and an undergraduate project by K. Lim. We would like to thank Department of Spatial Sciences at Curtin University of Technology, Institut für Photogrammetrie und Fernerkundung at Universität Karlsruhe and Prof. Dr.-Ing. Maria Hennes.

### REFERENCES

Büttgen, B., T. Oggier, M. Lehmann, R. Kaufmann, and F. Lustenberger, 2005. CCD/CMOS Lock-In Pixel for Range Imaging: Challenges, Limitations and State-of-the-Art. In: Proceedings of 1<sup>st</sup> Range Imag. Res. Day, pp. 21-32.

Gordon, S. J., 2005. Structural deformation measurement using terrestrial laser scanners, PhD thesis, Department of Spatial Sciences, Curtin University of Technology, 229 pages.

Kahlmann, T., Remondino, F. and Ingensand, H., 2006. Calibration for increased accuracy of the range imaging camera swissranger. In: Proceedings of the ISPRS Commission V Symposium 'Image Engineering and Vision Metrology', Dresden, Germany

Karel, W., P. Dorninger, and N. Pfeifer, 2007. In situ determination of range camera quality parameters by segmentation, In: Proceedings of International Conference on Optical 3-D Measurement Techniques, pp. 109 – 116.

Lange, R., 2000. 3D Time-of-flight distance measurement with custom solid state image sensors in CMOS/CCD-technology, University of Siegen, Department of Electrical Engineering and Computer Science, Germany

Mesa Imaging, 2008. <http://www.mesa-imaging.ch/>, accessed on March, 2008.

Oggier, T., M. Lehmann, R. Kaufmann, M. Schweizer, M. Richter, P. Metzler, G. Lang, F. Lustenberger and N. Blanc. 2003. An all-solid-state optical range camera for 3D real-time imaging with sub-centremeter depth resolution (SwissRanger), In: Proceedings of SPIE, vol. 5249, pp. 534-545.

Oggier, T., B. Büttgen, F. Lustenberger, G. Becker, B. Rügg, and A. Hodac. 2005. SwissRanger SR3000 and First Experiences based on Miniaturized 3D-TOF Cameras, In: Proceedings of 1<sup>st</sup> Range Imag. Res. Day, pp. 97-108.

Weingarten J., G. Gruener and R. Siegwart, 2004. A state-of-the-art 3D sensor for robot navigation, In: Proceedings of the IEEE/RSJ International Conference on Intelligent Robots and Systems, pp. 2155 – 2160.